

Exploring Site Response in the Taipei Basin with 2D and 3D Numerical Simulations

J. Miksat¹, K.-L. Wen², Ch.-T. Chen², V. Sokolov¹ and F. Wenzel¹

¹ *Geophysical Institute, Karlsruhe University, Hertzstr. 16, 76187 Karlsruhe, Germany,
joachim.miksat@gpi.uni-karlsruhe.de*

² *Institute of Geophysics, National Central University, No. 300, Jhongda Rd.
Jhongli City, Taoyuan County 32001, Taiwan (R.O.C)*

ABSTRACT :

The city of Taipei in northern Taiwan is located on a sedimentary basin and was affected by several destructive earthquakes in the past. Recent analysis of recorded data showed significant difference between records for deep and shallow events. Spectral amplifications for stations in the central part of the basin are larger for shallow than for deep earthquakes in the low frequency range ($f < 2$ Hz - 3 Hz). For stations located directly along the basin edges, no clear difference is observable.

We apply 3D finite-difference (FD) modelling of wave propagation in order to understand the observed peculiarities. The influence of deep and shallow earthquakes and of earthquake azimuth is explored by simulating incident S-wave front with varying incidence angles and azimuths. Furthermore, we explore 3D basin effects and evaluate the applicability of 2D numerical modeling of wave propagation for the Taipei basin by comparing simulations for 2.5D and 3D structures of the basin.

We show that numerical modeling can reproduce the spectral amplification characteristics found by analysis of recorded data. We found that 3D basin effects occur at the western deep part of the basin for deep and shallow earthquakes. In the eastern part of the basin 3D effects occur only for shallow earthquakes. Our studies suggest that 3D numerical modeling is an appropriate tool to simulate ground motion parameters for the Taipei basin in the low frequency range. As bridges and high-rise buildings are very sensitive to this low frequency part such a modeling is very important.

KEYWORDS: basin effects, spectral amplification, wave propagation, numerical modeling, finite-difference method, 3D effects

1. INTRODUCTION

The city of Taipei in northern Taiwan is located on a sedimentary basin and was affected by several destructive earthquakes in the past. As the seismicity of Taiwan is very high and the Taipei basin area is covered with a dense strong motion network, which is operated in the frame of the TSMIP (Taiwan Strong Motion Instrumentation Program) conducted by the CWB (Central Weather Bureau), a detailed analysis of observed ground motion can be performed. Recent analysis of this data showed significant difference between records for deep and shallow events. Chen *et al.* (pers. comm., 2008) showed that the H/V ratios for stations in the central part of the basin are larger for shallow than for deep earthquakes in the low frequency range ($f < 2$ Hz - 3 Hz). For stations located directly along the basin edges, no clear difference is observable. When comparing shallow earthquakes of different azimuths, the resulting H/V ratios in the low frequency range differ clearly at some stations. Sokolov *et al.* (2008a, 2008b) calculated the spectral ratios between a VHR (very hard rock) model and the actual observed records. The results also show that the spectral ratios for stations in the central part of the basin are larger for shallow than for deep earthquakes for frequencies up to 3 Hz.

We apply 3D finite-difference (FD) modelling of wave propagation in order to understand the observed peculiarities. Wave propagation through the Taipei basin is simulated for an incident S-wave front with varying incidence angles and azimuths in order to explore the influence of deep and shallow earthquakes and of earthquake azimuth. By comparing 3D and 2.5D modeling we explore the influence of 3D basin effects and

evaluate the applicability of 2D simulation of wave propagation for the Taipei basin.

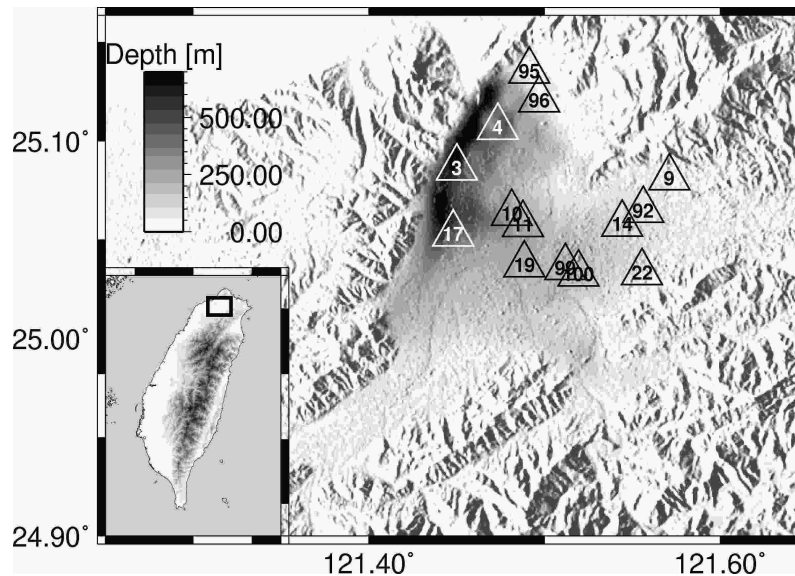


Figure 1: Map of the triangle shaped Taipei basin in northern Taiwan. The depth to the Tertiary basement is indicated by the grayscale. Triangles mark strong motion stations of the TAP network that are evaluated in this paper.

2. NUMERICAL MODELING OF WAVE PROPAGATION

2.1. Finite-Difference Modeling

We use a 3D FD method in order to simulate wave propagation for the Taipei basin (Furumura and Chen, 2005; Furumura *et al.*, 2003). The code is 4th (vertical direction) to 16th (horizontal direction) order in space and second order in time. 3 grid points per minimum wavelength in horizontal and 6 grid points per minimum wavelength in vertical direction are needed in order to obtain accurate results. Consequently, based on the minimum shear wave velocity and grid spacing (see section 2.2.), maximum frequency of our simulations is 1 Hz. At the sides and the bottom of the model damping and one-way absorbing boundary conditions are applied. The free surface is implemented by using the vacuum formulation, which allows to include topography.

In order to explore the Taipei basin response, we simulate planar S-wave front incidence on the basin for different incidence angles, which correspond to different earthquake depths. We also explore the azimuth dependence of the basin response by simulating wave front incidence for different azimuths. For each source grid point of the planar wave front, a double couple source is applied so that a pure S-wave front results in propagation direction. The resulting S-wave polarization of the source depends on the actual choice of the applied moment tensor components. In this paper we simulate wave propagation for SH-polarized wave fronts. The source time function of the added stress glut (Miksat *et al.*, 2008) at each grid point is described by a Herrman window with a width of 0.5 s. Deep earthquakes are described by a wave front incident from the bottom (incidence angle $i = 0^\circ$) and shallow earthquakes are simulated by incidence angles of 90° for different azimuths (90° and 180°). Polarizations of the source is in EW-direction for the deep earthquake and the shallow earthquake south of the basin. Polarization of the source is NS for the shallow scenario east of the basin.

We perform the simulations for two different subsurface structures, the developed Taipei basin model and a homogeneous model with $v_p = 3$ km/s, $v_s = 1.5$ km/s. These values correspond to the bedrock velocities in the Taipei basin model. Topography is included in both models. Frequency dependent spectral ratios are calculated by dividing the Fourier amplitude spectra (FAS) of the simulation with the basin structure by the FAS resulting from the simulation for the homogeneous model. Consequently, the spectral amplification show the effects of

basin geometry and the properties of the layers within the basin.

2.2. Subsurface Structure

The knowledge of the underground structure is essential for FD simulations of wave propagation. The structure of the Taipei basin is known from shallow reflection seismic experiments along many profiles through the city and on borehole drilling data (Wang *et al.*, 2004). The Taipei basin can be divided into a deep western and a shallow eastern part (Fig. 1). Based on the given depths of the Tertiary basement and the SRTM 90 m (CIAT, 2004) data, we constructed the sediment-bedrock boundary layer. From the data given in Wang *et al.* (2004), we calculated a velocity-depth function in order to assign proper P- and S-wave velocities for the basin. The minimum shear wave velocities of the uppermost layer, the so called Sungshan formation, is 170 m/s. Fig. 2 shows a slice through the created model. For the FD simulations the model is discretized with 50 m and 25 m in horizontal and vertical direction, respectively.

The horizontal (EW and NS) extensions of the model are 27.8 km to 27.8 km. Depending on the simulated scenarios, model depths vary between 2.6 km and 12 km.

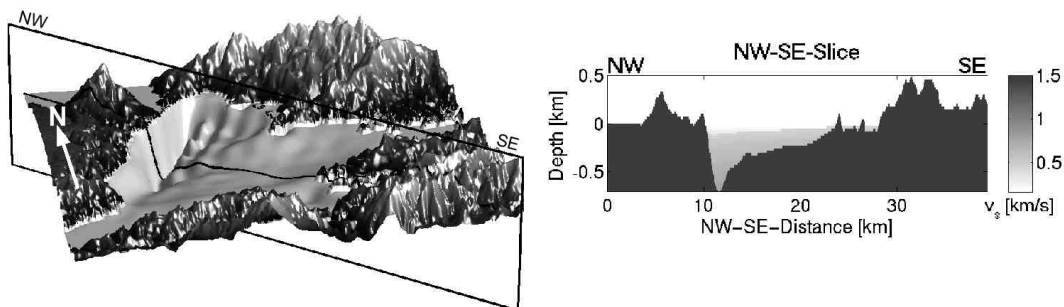


Figure 2: Left: Created topography-basement surface based on SRTM (CIAT, 2004) and Wang *et al.* (2004).
Right: NW-SE slice through the model.

3. SPECTRAL AMPLIFICATIONS

3.1. Deep and Shallow Earthquakes

We compare the basin response of an incident planar S-wave front from the bottom (deep earthquake) with a vertically incident wave front from the East (shallow earthquake).

In Fig. 3 spectral amplifications are given for stations in the western deepest part of the basin, the central part and for stations at the basin edge. Because of the polarization of the source (see section 2.1), we calculate spectral amplifications for the deep scenario from the EW-component and for the shallow scenario from the NS-component. For all stations within the western and central basin spectral amplification are larger for shallow earthquakes. However, along the basin edges the difference of spectral amplifications is very small. This behavior was also found by Sokolov *et al.* (2008a, 2008b) and Chen *et al.* (pers. comm., 2008). Amplification vary between 1 and 15, which is the same range as derived by Sokolov *et al.* (2008a, 2008b). Maximum amplifications for shallow earthquakes occur for stations at the deepest part of the basin at about 0.3 – 0.4 Hz and in the central part at 0.4 – 0.7 Hz. The same frequency dependence of the maximum amplification can also be seen in the VHR studies performed by Sokolov *et al.* (2008a, 2008b).

Fig. 4 shows snapshots of the wave propagation for an incident wave front of 90° from the East. The snapshots

show clearly the generation of surface waves at the eastern basin edges. Strong surface waves are excited at the eastern edge and at the eastern rim of the northern embayment of the basin and travel to the western deepest part of the basin. The waves generated at the eastern edge of the basin are guided mainly along a relatively deep channel to the West. The snapshots reveal that the basin edge generated surface waves are fully developed in the central part of the basin and therefore explain that spectral amplification for shallow earthquakes is larger than for deep earthquakes in the central part of the basin and that almost no differences can be observed near the basin edges.

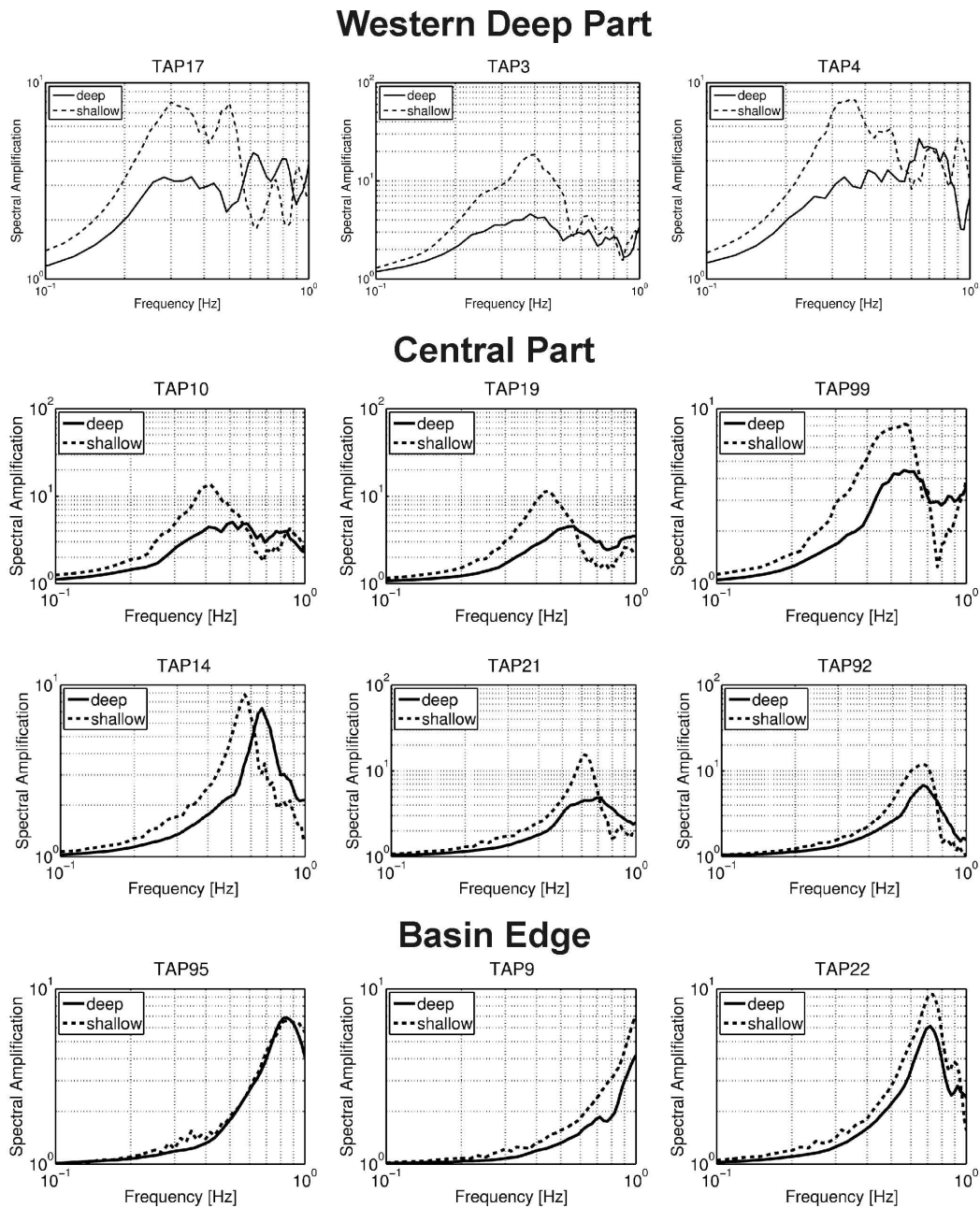


Figure 3. Modeled spectral amplification for the shallow and deep scenario. For stations in the western and central part, the amplifications of the shallow scenario are clearly larger than for the deep event. Maximum amplification occurs for stations at the deepest part at 0.3 Hz to 0.4 Hz, and for stations in the central part for 0.4 Hz to 0.6 Hz. For stations at the basin edge, spectral amplifications are similar for the deep and shallow scenario.

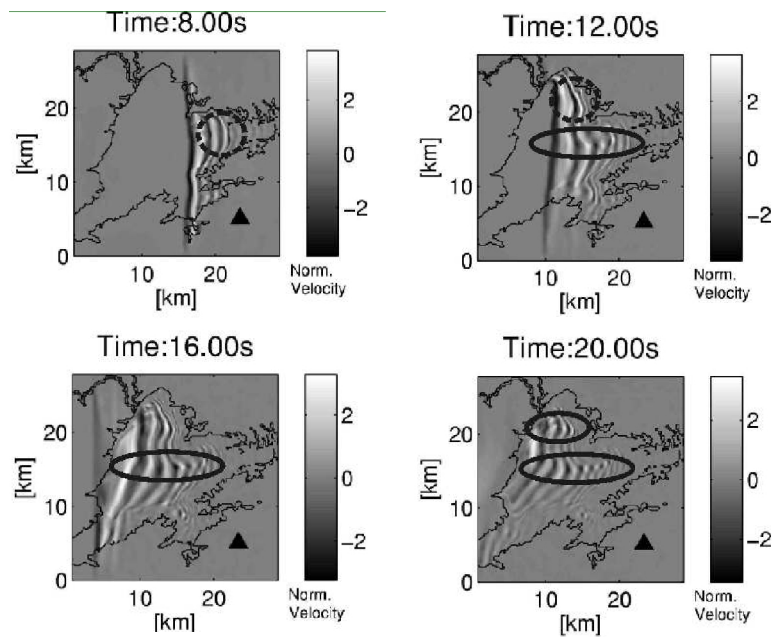


Figure 4: Snapshots of the wave field for wave incident of a shallow earthquake in the East. Surface waves are generated in the marked areas (dashed circles) and travel along the solid marked paths. Velocity is scaled to the PGV at the marked station outside the basin (black triangle).

3.2. Azimuth Dependence

Next, we compare the azimuth dependence of the Taipei basin response for shallow earthquakes south and east of the basin. For stations in the central part of the basin (TAP4, TAP11, TAP100) there is almost no difference between the two azimuths. Because of the generated surface waves, stations at the eastern edges of the basin (TAP96, TAP92) show larger spectral amplifications for earthquakes in the East and TAP17, located at the south-western edge, shows larger amplification for earthquakes in the South.

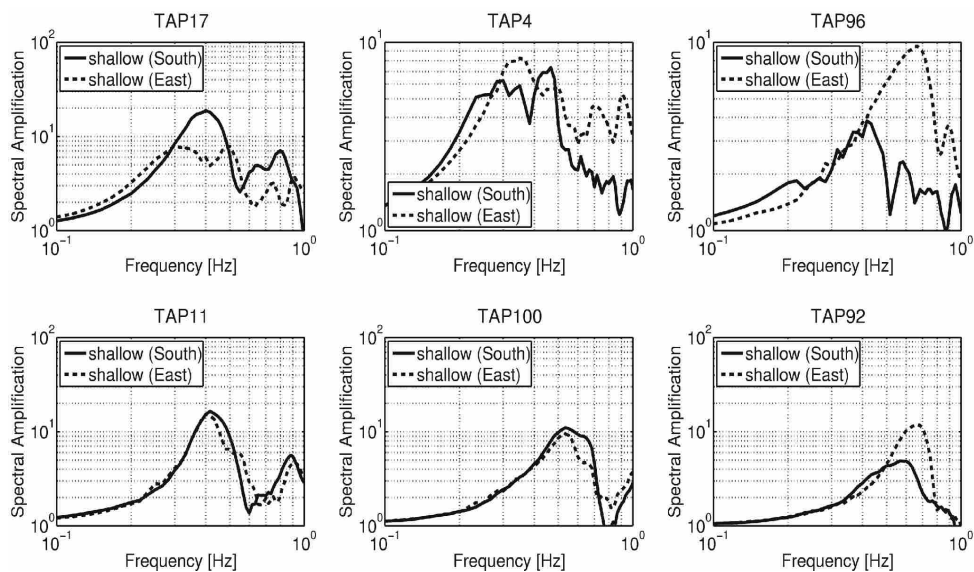


Figure 5: Modeled spectral amplification for shallow earthquakes south and east of the basin.

4. INFLUENCE OF THE 3D BASIN STRUCTURE

In order to explore the influence of 3D basin effects we compare simulations of wave propagation for the 3D subsurface model with a 2.5 D model of the Taipei basin. Fig. 6 shows the 3D basin model and the corresponding 2.5D model of an EW slice through the 3D structure for NS-distance equal to 22.8 km indicated by the three stations (triangles). We simulate an incident S-wave front from the bottom for the 2.5D model and for the 3D structure and evaluate EW and NS components at the three indicated stations (Fig. 7). As the input motion of the source is in EW direction there is almost no NS motion observable for the 2.5D model (small values are obtained because of the finite size of the incident planar S-wave front) and the resulting ground motion on the NS component of the wave propagation simulation through the 3D subsurface structure indicates the influence of the 3D basin structure. At all three stations the modeling for the 3D subsurface structure yield to clearly visible NS-components compared to the 2.5D modeling. For the station at 10.2 km and 12.2 km the amplitude of the NS component is about 30 % of the amplitude of the EW component. For the station at EW-position of 14.9 km the effect of the 3D structure is less than 20 %.

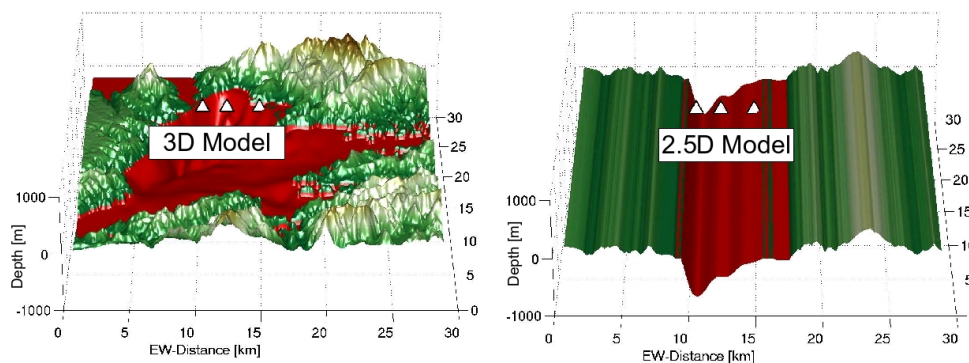


Fig. 6: 3D model of the Taipei basin and a 2.5D model which is generated from an EW-slice through the 3D structure at NS-distance equal to 22.8 km indicated by the receiver positions in the 3D model (triangles).

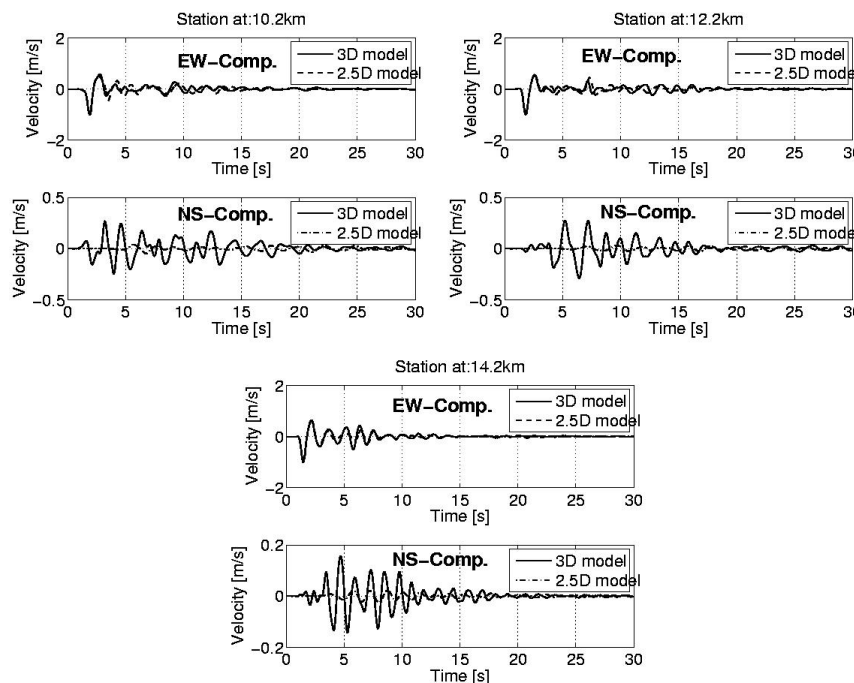


Fig. 7: Resulting ground motion of a deep earthquake for the 3D and 2.5D structures at the stations shown in Fig. 6. The velocities are scaled to the maximum of the EW component of the simulation within the 3D structure. The NS-component indicates the influence of the 3D structure of the basin.

The influence of the 3D basin structure can also be seen in the PGV (Peak Ground Velocity) distribution of the EW and NS components. For the deep scenario shown in section 3.1. the PGV of the EW and NS components are displayed in Fig. 8. All values are scaled to the maximum of the EW-component at a reference station (black triangle). As the source component is pure EW motion, PGV of the NS component is an indicator of the influence of the 3D basin structure. The largest amplitudes of the NS-component occur in the northern deep part of the basin. In the shallow eastern part of the basin only small PGV values are obtained for the NS-component. This suggests that 2D modeling of wave propagation can be applied in order to simulate ground motion in the eastern shallow part for deep earthquakes and not in the western deep part of the basin where the NS-amplitude generated by 3D effects is more than 50% of the EW-amplitude.

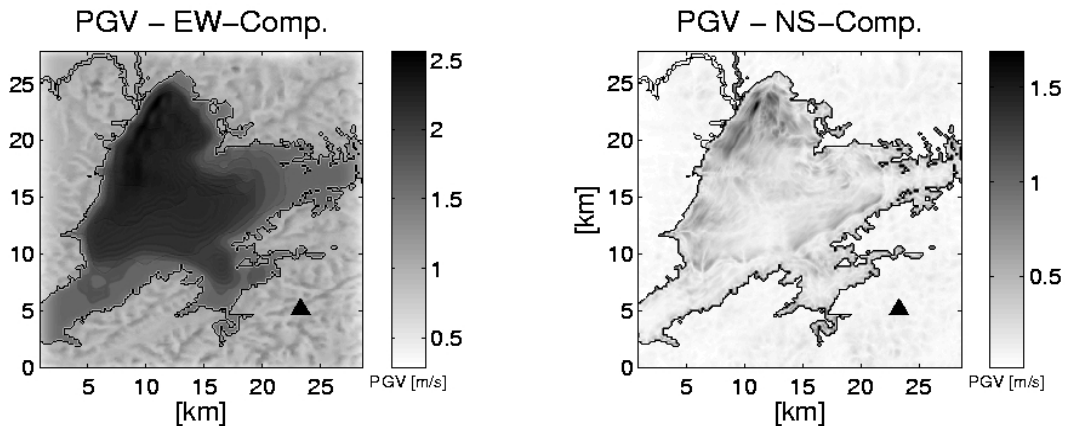


Fig. 8: PGV of the EW- and NS-components for a deep earthquake. The source component is EW orientated. Therefore, PGV of the NS-component shows the influence of the 3D basin structure. All values are scaled to the maximum of the EW-component at a reference station (black triangle).

Fig. 9 displays the PGV distributions of the horizontal components for the shallow scenario east of the basin discussed in sections 3.1 and 3.2. In this case the source component is pure NS and the PGV of the EW-component is an indicator of the influence of the 3D basin structure. All values are scaled to the maximum of the NS-component at the indicated reference station (black triangle). Again the western deep part show large amplitudes produced by 3D effects. Especially at the central part of the western basin edge PGV of the EW- and NS-components have about the same amplitude, but large PGV of the EW-component are also obtained in the eastern shallow part. Especially along the wave guide the surface waves travel to the West (see Fig. 4 and discussion in section 3.1). This indicates that the application of 2D modeling in order to calculate ground motion is not applicable for shallow earthquakes for the whole basin area.

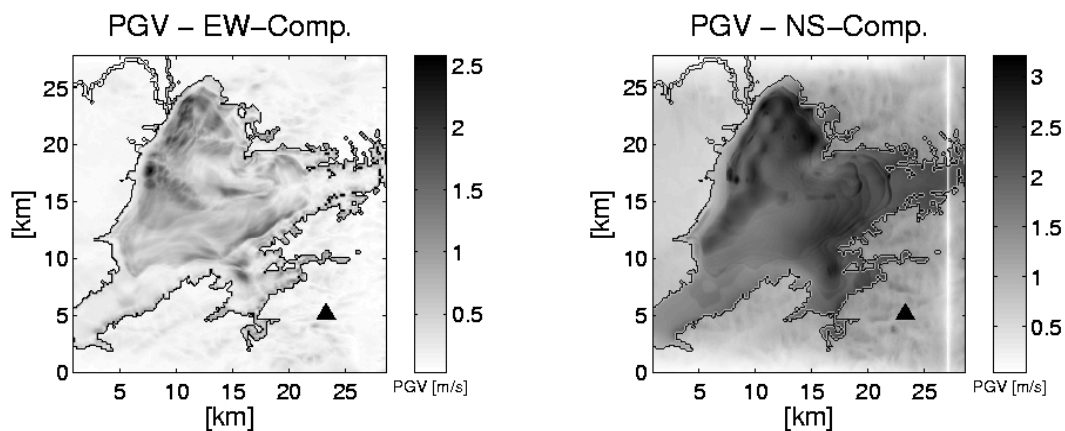


Fig. 9: PGV of the EW- and NS-components for the shallow scenario east of the basin. The source component is NS orientated. Therefore, PGV of the EW-component shows the influence of the 3D basin structure. All values are scaled to the maximum of the NS-component at the indicated reference station (black triangle).

5. CONCLUSIONS

By applying FD simulations of wave propagation for an incident planar S-wave front on the Taipei basin, we reproduced spectral amplification characteristics derived from analysis of observed data (Sokolov et al, 2008, 2008b, Chen *et al.*, pers. comm., 2008). We showed, that the strong amplifications for shallow earthquakes in the low frequency range can be attributed to the generation of surface waves at the basin edges. Furthermore, the modeling underlines the strong azimuth dependence of the resulting ground motion for shallow earthquakes. Our studies suggest that modeling can be useful to extend the observed data base for areas where the station network is not dense. As high-rise buildings and high-way bridges are sensitive to the considered low frequency range, such simulations are very important.

We showed that the influence of the 3D basin structure is important in the western deep part of the basin for deep and shallow earthquakes. We found that ground motion in the eastern shallow part of the Taipei basin can be simulated by 2D numerical modeling for deep earthquakes. In contrast, ground motion generated by shallow earthquakes produce large surface waves that are guided along paths controlled by the 3D structure of the basin. Therefore, 2D modeling is not applicable in order to calculate accurate ground motions for shallow earthquakes for the whole Taipei basin area.

ACKNOWLEDGEMENTS

We thank Takashi Furumura for providing is 3D Finite-Difference code. The simulations were performed on the HP XC6000 of the Scientific Super Computing Centre Karlsruhe. This research is funded by the Deutsche Forschungsgemeinschaft (DFG), Germany (project WE-1394/13-1) and the NSC (National Science Council), R.O.C (grant NSC 96-2119-M-008-007).

REFERENCES

- CIAT (2004). Void-filled seamless SRTM data V1, 2004, International Centre for Tropical Agriculture (CIAT), available from the *CGIAR-CSI SRTM 90m Database*: <http://srtm.csi.cgiar.org>.
- Erdik, M. and Durukal, E. (2003). Simulation Modeling of Strong Ground Motion in Chen, W.-F. and Scawthorn (editors), *Earthquake Engineering Handbook*, CRC Press, Boca Raton, London, New York, Washington D.C.
- Furumura, T., and L. Chen (2005). Parallel simulation of strong ground motions during recent and historical damaging earthquakes in Tokyo. Japan, *Parallel Comput.*, **31** 149–165.
- Furumura, T., B.L.N. Kennett, and K. Koketsu (2003). Visualization of 3D wave propagation from the 2000 Tottori-ken Seibu, Japan, earthquake: observation and numerical simulation. *Bull. Seism. Soc. Am.* **93** 870–881.
- Miksat, J., Müller, T. M. and Wenzel, F. (2008). Simulating three-dimensional seismograms in 2.5-dimensional structures by combining two-dimensional finite difference modelling and ray tracing. *Geophysical Journal International* **174**:1 309-315.
- Sokolov, V., Wen, K.-L., Miksat, J., Wenzel, F., Chen C.-T. (2008a). Analysis of Taipei basin response on earthquakes of various depth and location using empirical data. *31st General Assembly of the European Seismological Commission ESC 2008*, Hersonissos, Crete, Greece (submitted).
- Sokolov, V., Wen, K.-L., Miksat, J., Wenzel, F., Chen C.-T. (2008b). Analysis of Taipei basin response on earthquakes of various depth and location using empirical data. *Terr. Atmos. Ocean. Sci.* (submitted).
- Wang C-Y, Lee Y-H, Ger M-L, and Chen Y.-L. (2004). Investigating subsurface structures and P- and S-wave velocities in the Taipei Basin. *Terr. Atmos. Ocean. Sci.*, 15:4 609–627.